Polymer 163 (2019) 171–177

Contents lists available at ScienceDirect

Polymer

journal homepage: www.elsevier.com/locate/polymer

Interfacial structures and mechanisms for strengthening and enhanced conductivity of graphene/epoxy nanocomposites

W. Zheng[a], W.G. Chen[a,*], Q. zhao[a], S.X. Ren[a], Y.Q. Fu[b,**]

[a] School of Materials Science and Engineering, Xi'an University of Technology, Xi'an, Shaanxi, 710048, PR China
[b] Faculty of Engineering and Environment, Northumbria University, Newcastle upon Tyne, NE1 8ST, UK

HIGHLIGHTS

- Graphene/epoxy nanocomposite was successfully prepared via *in-situ* polymerization.
- Aliphatic ether bonds were formed between graphene and epoxy resin matrix.
- The composite showed significantly improved mechanical properties and conductivity.
- Enhancement mechanisms are effective transfer of stress and bridging of graphene.

ARTICLE INFO

Keywords:
Graphene
Nanocomposites
Mechanical properties
Interface characterization

ABSTRACT

Graphene/epoxy resin nanocomposites were prepared using an *in-situ* polymerization process, and their formation mechanisms, microstructures, mechanical properties and electrical conductivity were characterized. Results showed that graphene is well dispersed in the epoxy matrix, and covalent cross-links are formed between graphene and epoxy matrix. Tensile strength and modulus of the graphene/epoxy composites were found to increase firstly and then decrease with the increase of graphene loading contents. When the graphene content was 0.3 wt%, tensile strength, tensile modulus and elongation were found to increase by 46.8%, 47.3% and 24.0% compared with those of pure epoxy resin. When the graphene content was 1.38 vol%, the conductivity of the composite was 3.28×10^{-4} S m^{-1} with a low percolation threshold of 0.47 vol%. Enhancement mechanisms for the properties of composites were identified to be dispersion strengthening, effective transfer of stress and bridging of graphene.

1. Introduction

Epoxy resin is one of the commonly used thermosetting resins for wide-range applications including adhesives, insulation materials and coatings in various fields such as electronics, electrical appliance and aerospace industry due to its good mechanical properties, bonding properties and chemical stability [1,2]. However, pure epoxy resin is an insulator, which can accumulate static charges during its applications, and severe electrostatic discharge can cause personal electric shock, electronic device failure and even explosions in some extreme cases. Therefore, it is crucial to modify the epoxy resin, for example, using conductive nanofillers, to prevent this issue and simultaneously enhance its mechanical and physical properties [3,4].

Graphene, a mono-atomic layer consisting of sp^2 hybridized carbon atoms [5], has received significant attention as the nanofillers due to its superior properties, such as electrical conductivity (~10^8 S m^{-1}), tensile strength (~130 GPa), Young's modulus (~1.0 TPa), thermal conductivity (~5000 W·m^{-1}·K^{-1}), and large specific surface area (~2600 m^2/g) [6–8]. Adding tiny amounts of graphene as the filler can significantly improve the performance of epoxy based composites [9]. For example, Li et al. [10] added 3 wt% of graphene nanosheets into the epoxy, and the electrical conductivity of epoxy resin-based graphene composites was 10^2 S/m, and the tensile strength was 78 MPa, significantly higher than those of the pure epoxy resin (e.g., 13 orders of magnitude improvement in conductivity and 20% in tensile strength). Liu et al. [11] prepared a three-dimensional (3D) network structure of composites using foamed graphene inside the epoxy resin. They reported that when the amount of graphene was 5 wt%, the electrical conductivity of the composite was increased by 12 orders of magnitude, up to a value of 10^{-2} S/m. The strong π-π interactions among the

* Corresponding author.
** Corresponding author.
E-mail addresses: wgchen001@263.net (W.G. Chen), richard.fu@northumbria.ac.uk (Y.Q. Fu).

https://doi.org/10.1016/j.polymer.2018.12.055
Received 11 August 2018; Received in revised form 23 November 2018; Accepted 30 December 2018
Available online 04 January 2019
0032-3861/

graphene sheets make them tend to be adsorbed or agglomerated in the composite matrix [12]. Therefore, it is a critical issue to disperse the graphene materials uniformly inside the polymer matrix.

The most commonly used method for improving the dispersibility of graphene is to introduce chemical functional groups to modify the surfaces of the graphene sheets. For example, Chen et al. [13] used poly (2- butylaniline) (P2BA) as a dispersing agent and achieved a stable dispersion of graphene in organic solvents via non-covalent π-π interactions between P2BA and graphene nanosheets. Yao et al. [14] reported that a homogeneous dispersion of graphene nanosheets in the epoxy can be obtained via chemical functionalization of graphene oxides with 4-nitrobenzenediazonium salt. However, it should be pointed out that many functional groups on the modified graphene will influence the initiation and growth reactions of the matrix polymerization chains. It was also reported that with the appropriate preparation methods such as *in situ* polymerization, graphene can achieve a homogeneous dispersion in the polymer matrix [15–17].

Currently research on graphene/epoxy composites is mainly focused on how to evenly distribute the graphene in the polymer matrix to improve the conductivity and mechanical properties of the composites. The two-phase interfaces in the composite material have an interfacial layer with a considerable thickness, and due to this interfacial effect, the reinforcement could be easily formed within the resin matrix. These interfaces effectively prevent the propagation of cracks in the matrix, or consume much more external energy for the crack's propagation [18]. Graphene has an atomic layer thickness and also an ultra-high specific surface area, which is very effective in forming multiple interfaces [19]. Although there are many studies on the interfacial bonding strength and mechanical behavior of the graphene-reinforced polymer composites, it is relatively less investigated for the interfacial microstructures between the graphene and epoxy.

In this work, graphene/epoxy resin composites were prepared using an *in-situ* polymerization method with graphene as the reinforcement agency. The interfacial structures of graphene/epoxy were characterized, and tensile and electrical properties of the composites were tested. Finally, the enhancement mechanisms of the composites were discussed.

2. Experimental

2.1. Raw materials

The graphene used in this work was prepared using a chemical reduction method which has been reported in our previous article [20]. Epoxy monomers (bisphenol A type, E-44) and curing agent (polyamide resin, 650) were bought from Nantong Xingchen Material Synthesis Co., Ltd, China, with their key features listed in Table 1.

2.2. Preparation of composites

Fig. 1 illustrates the in-situ polymerization process to fabricate graphene/epoxy resin nanocomposites. Firstly, epoxy monomer and polyamide curing agent were mixed with a ratio of 2:1. Then the epoxy resin monomer of 5 g was diluted with an excessive amount of absolute ethyl alcohol for easy stirring. According to the total mass percentages of epoxy monomer and curing agent, 0 wt%, 0.1 wt%, 0.3 wt%, 0.5 wt %, 0.8 wt%, 1.0 wt%, 1.5 wt%, 2.0 wt%, and 2.5 wt% of graphene were added into the absolute ethyl alcohol, and ultrasonically dispersed for 20 min. The so-formed graphene dispersion was mixed with the prepared epoxy resin solvent, and further ultrasonically dispersed at 50 °C for 1 h. The mixture was placed in an oven and dried at 80 °C for 1 h to volatilize the anhydrous ethanol, then was transferred into a vacuum oven at 80 °C for 2 h to remove bubbles and remaining anhydrous ethanol. The polyamide resin was then added inside the prepared epoxy, and the mixture was slowly stirred to prevent formation of air bubbles. The prepared graphene/epoxy resin composite was cast in a mold pre-coated with silicone oil, and the mold was placed in an oven at 70 °C and cured for 8 h before the demolding process.

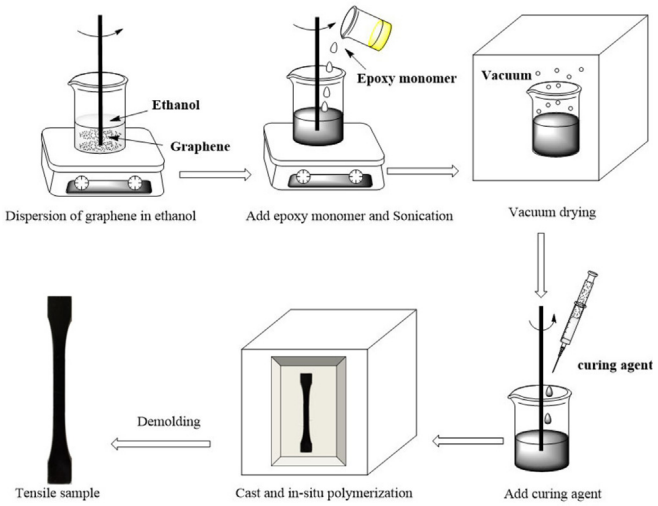

Fig. 1. Illustration of preparation process of graphene/epoxy nanocomposites.

2.3. Characterization

Fourier-transform infrared spectroscopy (FTIR) was used to characterize the epoxy resins before and after the graphene were added. Based on the results obtained using a TENSOR 27 FT-IR spectrometer, the functional group changes of the epoxy resin and the chemical bonds between the graphene and the epoxy matrix were analyzed [21]. The sample was ground into powders and mixed with KBr powder, then pressed at 80 MPa before testing. The scan range of the wave number was 4000 cm^{-1}-400 cm^{-1} with a resolution of 4 cm^{-1}.

The force-distance curve of the indentation tests was obtained using a Bruker Dimension FastScan atomic force microscope with an RTESPA-525 probe. Mechanical properties of the nanocomposites were tested using WEW-C universal testing machine. The size of tensile sample was 150 × 20 × 4 mm. Fracture morphology was observed using a TESCAN VEG3XMU scanning electron microscope (SEM). The composites with 0 wt% ~ 0.8 wt% graphene were cut into a 50-nm-thick slice using a cryo-ultramicrotome machine, and microstructures and distributions of graphene inside epoxy resin were characterized using a high resolution transmission electron microscope (HR-TEM, FEI-Talos F200X).

Electrical conductivity of the moderately conductive composites (resistance value $\leqq 10^8\Omega$) was measured using a VersaLab comprehensive physical property measuring system. For the pure epoxy and composites with a low conductivity value (e.g., resistance value $> 10^8\Omega$), the conductivity testing was performed using an ATI-212 ultrahigh resistance meter. The sample to be tested was made into a sheet form with an area of 10 × 10 mm and a thickness less than 2 mm. The sheet resistance values were measured, and the resistivity value

Table 1
Key properties of commercial epoxy monomers.

Indicator	Epoxy equivalent/eq	Softening point/°C	Room temperature viscosity/Pa·S	Inorganic chlorine/ppm	Volatiles/%
Data	210–244	15–23	6–10	≤200	≤1.0

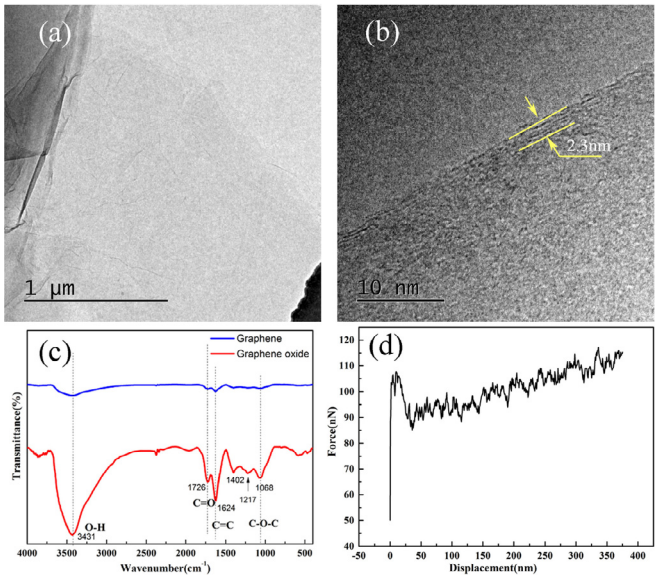

Fig. 2. (a) TEM image of raw graphene; (b) HR-TEM image of graphene; (c) FT-IR spectra of graphene and graphene oxide; (d) Force-distance indentation curve for graphene obtained from AFM analysis.

was calculated by multiplying the thickness of the sheet.

3. Results and discussion

3.1. Microstructures of graphene and graphene/epoxy resin composites

Fig. 2(a) shows a typical TEM image of graphene prepared using the chemical reduction method [20]. It can be seen that the graphene shows wrinkled structures which were caused by the removal of functional groups during de-oxygenation process. Fig. 2(b) shows an HR-TEM image of the graphene. The graphene sheet has a thickness of about 2.3 nm and a single layer of carbon atoms has a thickness of 0.35 nm, which indicates that the graphene prepared is a few layer thick [22]. Fig. 2(c) is an FT-IR spectrum of graphene. It can be seen that the graphene sample retains some oxygen-containing functional groups such as hydroxyl group, carboxyl group and epoxy group, respectively, with a dominant hydroxyl group compared with the epoxy group. Fig. 2(d) shows the force-distance curve of the graphene obtained from the indentation test. The measured and calculated elastic modulus of graphene layer is about 1.033 TPa.

Fig. 3 shows TEM images of the pure epoxy resin and the composite with 0.5 wt% graphene. According to polymer matrix composite theory [18], the curing reaction of the epoxy resin extends radially from the center of the curing agent to its periphery, and as a result, a non-uniformly solidified structure with a dense center area and a less-dense edge area is formed. The dense structure at the center area is often called micelle. The features of these micro-micelles have a significant contrast compared with the surrounding area in the TEM image of the pure epoxy resin as shown in Fig. 3(a). The darker area in Fig. 3(a) is the micro-micelles. It can be seen that the micro-micelles in the pure epoxy resin are randomly distributed. In the TEM image of the composite material, the background of micro-micelle and some black lines can be observed (see Fig. 3(b), (c) and 3(d)). The black lines are the images of the graphene sheet. The features are consistent with those of graphene/polymer composite reported in literature [23,24]. The width of the black lines in Fig. 3(d) was calculated to be about 2 nm, which is near the thickness of prepared graphene. This also shows that the black lines in Fig. 3(b)–(d) are multi-layered graphene. It can be seen from Fig. 3 that the graphene sheets are curved and interconnected with each other, indicating that the graphene is flexible and deformed/dispersed

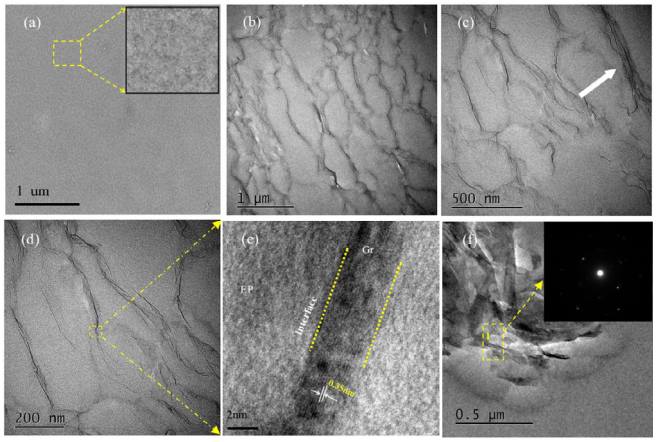

Fig. 3. (a) TEM image of pure epoxy resin; (b) to (d) TEM images of 0.5 wt% Gr/EP at different magnifications; (e) HR-TEM of interfacial region between graphene and epoxy; (f) TEM image showing the morphology of the graphene sheet in the composite; inset is the SAED pattern of position.

in the epoxy resin.

The properties of polymer-based nanocomposites are significantly affected by the dispersion and interfacial bonding of the nano-fillers inside the polymer matrix. In Fig. 3(b) and (c), most graphene sheets are uniformly distributed inside the matrix without any preferred orientation. However, some of these sheets are agglomerated together, which may affect the mechanical properties of the composites, and these are closely linked with the tensile test results (which will be discussed later). The white arrows in Fig. 3(c) indicate the graphene agglomerates observed in the composite.

Fig. 3(e) is an HR-TEM image of the interface between graphene and epoxy resin. The interfacial layer is dense without apparent voids, indicating that the matrix has a good wetting property with the surface of graphene. This is because the surface tension of the graphene (129 dyn/cm [25]) is higher than that of the epoxy resin (43 dyn/cm [26]), and the interfacial region forms a dense layer. In the curing processes of the composite, the micro-micelles tend to be arranged in an aligned pattern due to the action of the surface molecules of the graphene, thereby changing the microstructure and density of the interfacial layer. Compared to Fig. 3(a) and (e) shows that the micro-micelles near the graphene region tend to be highly aligned.

Fig. 3(f) shows the planar morphology of the graphene sheet in the composite material. The graphene sheet is folded inside the epoxy resin matrix and the layer is quite thick, showing its agglomerated pattern. Fig. 3(f) also shows the selected area electron diffraction pattern at position 1 in Fig. 3(f), which is a typical hexagonal diffraction pattern. This verifies the presence of graphene at this location, which has also been widely reported in literature [27–29].

Based on the TEM observation, the graphene has been well dispersed in the epoxy resin matrix. Because they were chemically cross-linked using the aliphatic ethers (Fig. 4(b)), the chemical interactions between the graphene and the epoxy resin has been enhanced.

3.2. FT-IR spectroscopy analysis

Fig. 4(a) shows the FT-IR spectra of the epoxy resin before and after adding the graphene. It can be found that the epoxy resin after adding the graphene shows a new absorption peak at 1136 cm^{-1} compared with that of pure epoxy resin. Based on literature [30–33], this peak corresponds to the C—O stretching vibration mode of the aliphatic ether, indicating that there are aliphatic ethers existed in the composite material. In the *in-situ* polymerization process, the hydroxyl groups on the graphene react with the epoxy group on the epoxy monomer under the catalytic enhancement of the polyamine in the curing agent [34],

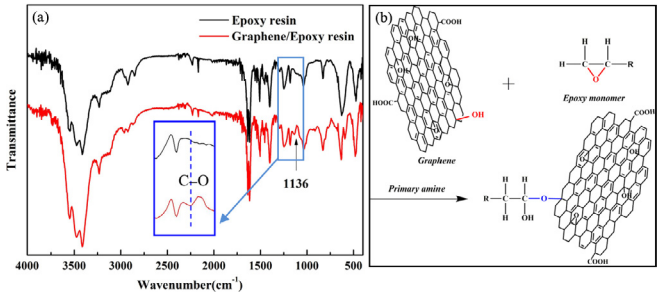

Fig. 4. (a) FT-IR spectra of the pure epoxy resin and 0.5 wt% nanocomposite; (b) reaction diagram of the *in-situ* polymerization process, in which the blue lines represent aliphatic ethers.

thus the aliphatic ether was formed, which can strongly bond the graphene and epoxy matrix. The detailed reaction process is illustrated in Fig. 4(b).

3.3. Mechanical properties

Fig. 5(a) shows the stress-strain curves of the composites during tensile testing with different mass fractions of graphene measured at room temperature. Only a small amount of plastic deformation occurs before the fracture of both the pure epoxy resin and the composites. Tensile strength, elastic moduli and elongations before the fracture of the composites with different graphene contents are shown in Figs. 5(b) and 5(c). As the content of graphene is increased, all the above data are firstly increased but then decreased afterwards. When the graphene loading is 0.3 wt%, the tensile strength and elastic modulus of the composite reach their maximum values. The modulus was increased from 1.82 GPa of the pure epoxy to 2.68 GPa of the composite (an increment of 47.3%). The tensile strength was increased from 46.5 MPa for the pure epoxy to 68.3 MPa for the composite (an increment of 46.8%). The elongation values of the composites were increased by 16.3% and 24.0%, compared with those of the pure epoxy resin, when the content of graphene in the composite is 0.1% and 0.3%, respectively. The existence of the optimum mechanical property of the composites at a certain graphene concentration has been widely reported in literature. For example, Zhang et al. [35] prepared graphene/epoxy resin composites and the best mechanical properties of the composites occurred at 0.3 wt% graphene. Ni et al. [36] prepared pyrolysis graphene/epoxy resin composites, and the tensile strength was maximized at a graphene concentration of 0.1 wt%.

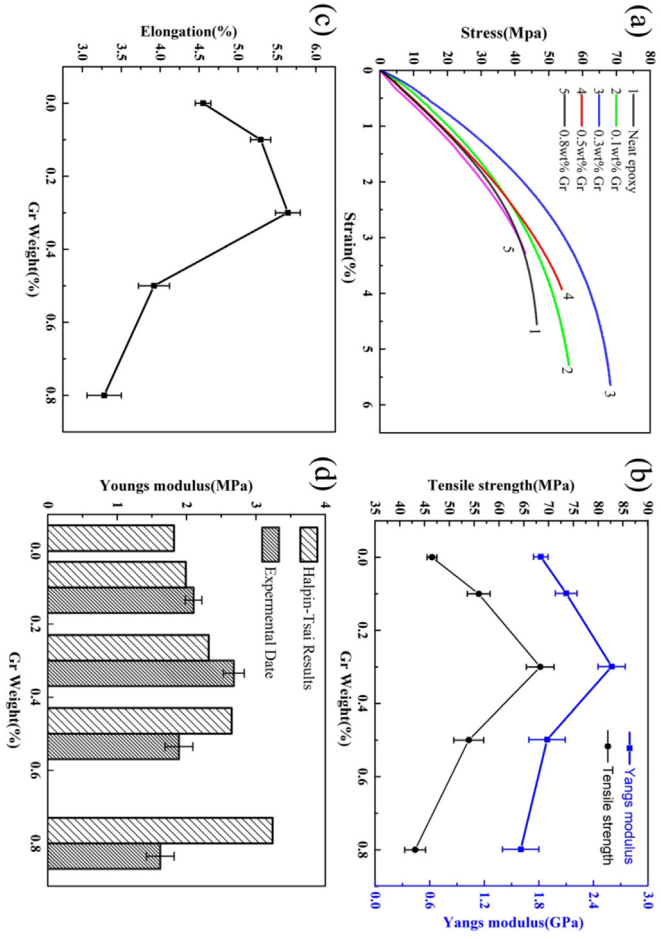

Fig. 5. (a) Tensile stress-strain curves for pure epoxy and epoxy nanocomposites; (b) to (c) tensile strength and elongation results for pure epoxy and nanocomposites; (d) comparison of theoretically predicted tensile moduli using the Halpin-Tsai theory and the experimentally obtained data.

Halpin-Tsai equation can be used to predict tensile moduli of the composites, and it has been successfully used for a variety of composite systems [37]. The Halpin-Tsai equations were modified for the graphene/epoxy nanocomposite as follows [38,39]:

$$E_C = \left(\frac{3}{8}\frac{1+\xi\eta_L V_f}{1-\eta_L V_f} + \frac{5}{8}\frac{1+2\eta_T V_f}{1-\eta_T V_f}\right) \times E_m \quad (1)$$

where the parameter η is given by:

$$\eta_L = \frac{(E_f/E_m)-1}{(E_f/E_m)+\xi} \quad (2)$$

$$\eta_T = \frac{(E_f/E_m)-1}{(E_f/E_m)+2} \quad (3)$$

where E_L is the longitudinal composite tensile modulus, E_T is the transverse composite tensile modulus, E_M is the tensile modulus of the EP, E_f is the tensile modulus of the graphene, V_f is the volume fraction of graphene. The volume fraction V_f, can be expressed as follows:

$$V_f = \frac{\omega_f}{\omega_f + (\rho_f/\rho_m)(1-\omega_f)} \quad (4)$$

where ω_f is the weight fraction of graphene, ρ_f is the graphene density, and ρ_m is the matrix density. ξ is the filler shape factor, which can be further expressed as:

$$\xi = 2\left(\frac{(W+L)}{t}\right) \quad (5)$$

where L, W, and t represent the average length, width, and thickness of the graphene. The density readings of the graphene and epoxy resin are 2.2 g/cm^3 and 1.2 g/cm^3. For this study, W ≈ 2 μm, L ≈ 3 μm, t ≈ 2.3 nm, E_f ≈ 1.033 TPa. The calculated results of tensile moduli for the composite materials are shown in Fig. 5(d). However, the Halpin-Tsai theory does not consider the aggregation phenomena, thus it fails to predict the moduli at higher loadings. At lower loadings, the experimental results are higher than those from the theoretical predictions. This may be due to the fact that the chemical bonding between graphene and the matrix further enhances the strength of the composite.

Fig. 6 shows SEM photographs of facture surfaces of the pure epoxy and the composite after the tensile test. It can be seen from Fig. 6(a) that the fracture morphology of pure epoxy shows typical cleavage patterns with a series of parallel steps on the fracture surface, which are roughly aligned along the crack propagation direction. With 0.3 wt% of graphene in the composite, the fracture morphology of the composite was changed significantly. As is shown in Fig. 6(b), the surface shows many bulges and fracture patterns, similar as tearing edges in a typical quasi-cleavage fracture. Due to the superior mechanical properties of graphene, during the fracture, the cracks will change their propagation routes when they encounter the graphene layers. There is a good

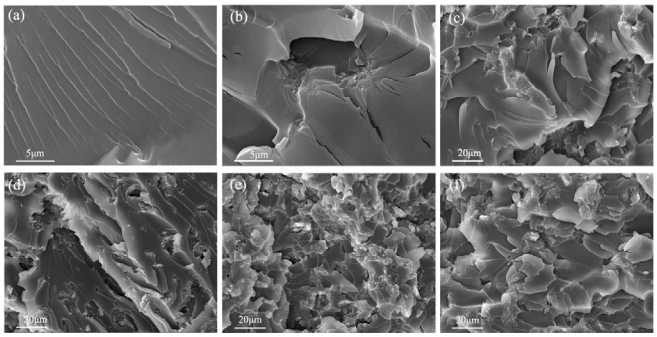

Fig. 6. SEM image of the fractured surfaces of pure epoxy and epoxy nanocomposites: (a) pure epoxy; 10000 × ,(b) 0.3 wt% graphene, 10000 × ; (c) 0.1 wt% graphene, 2000 × ; (d) 0.3 wt% graphene, 2000 × ; (f) 0.5 wt% graphene, 2000 × ; (f) 0.8 wt% graphene, 2000 × .

covalent bonding between graphene and epoxy resin, and the graphene could be pulled out from the matrix when it breaks, thus forming rough fracture patterns on the surface. This is consistent with the tensile properties of the composites that adding a small amount of graphene improves the strength of the epoxy resin. Fig. 6(c)-6(f) show the facture surfaces of graphene/epoxy resin composites with different graphene fractions. When the content of graphene is increased up to a certain value (e.g., 0.3 wt%), the fracture surface becomes very rough.

Based on the above results, if a small amount of graphene (e.g., less than 0.3 wt%) is added in the matrix, serious agglomeration phenomenon will not happen, and graphene is generally distributed uniformly in the matrix. Therefore, its 2D structure can effectively transfer the applied stress and hinder the propagation of cracks. It can be seen from the tensile test results shown in Fig. 5 that adding a small amount graphene can increase the strength and plasticity of the composite, which is similar to those reported in literature [14,35]. Simultaneously the oxygen-containing functional groups on the graphene surface are chemically bonded to the polymer matrix, thus forming a good interfacial bonding between the graphene and matrix. Under the external stress, the epoxy resin among the graphene sheets will be deformed and then broken, thus showing the rough fracture morphology (see Fig. 6(b)). Based on these discussions, the fracture failure mechanism of the composites is summarized in Fig. 7.

TEM images of graphene/epoxy nanocomposites with the different graphene loadings are shown in Fig. 8 and Fig. 3(d). It is apparent from the figure that as the graphene loading is increased, the number of black lines in the corresponding TEM image of the composites is

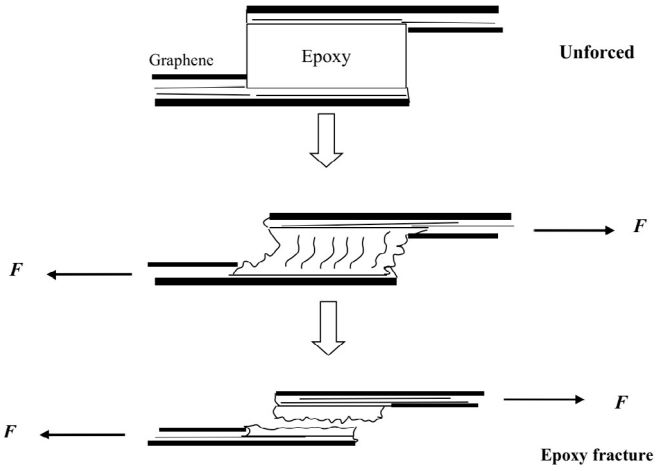

Fig. 7. Illustration of fracture failure mechanisms of graphene/epoxy composites.(Graphene transfer stress causes deformation and fracture of epoxy resin due to good interfacial bonding between the graphene and matrix.)

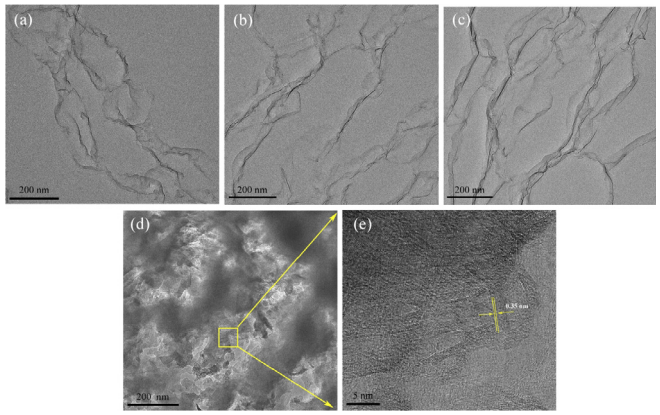

Fig. 8. TEM images of graphene/epoxy nanocomposites in different loadings; (a) 0.1 wt% graphene,(b) 0.3 wt% graphene,(c) to (d) 0.8 wt% graphene,(e) HR-TEM of graphene/epoxy nanocomposites loading of 0.8 wt%.

increased (see Fig. 8(a)-8(c) and Fig. 3(d)). When the graphene loading is increased to 0.8 wt%, in some areas the graphene is uniformly distributed (Fig. 8(c)), whereas in other areas, there are severely agglomerated structures observed (Fig. 8(d)). From the HR-TEM image of the agglomerated structure shown in Fig. 8(e), the lattice fringes of (001) crystal plane for the graphene can be clearly seen, and a large amount of graphene is agglomerated in this region. The local stress concentration generated in this area of the composite leads to the premature fracture under an external stress. It can be seen from Fig. 5 (b) and 5(c) that the strength and plasticity of the composite material are significantly reduced when the graphene content in the composite is larger than 0.3 wt%.

3.4. Conductivity analysis

The plots of conductivity readings versus filler content for the epoxy nanocomposites filled with graphene is shown in Fig. 9. It can be seen that the composite exhibits a percolation phenomenon [40], which will be explained as follows. When the graphene content is low (e.g., ≤0.20 vol%), the conductivity is only increased slightly with the volume fraction of the filler. However, when the volume fraction of graphene is increased from 0.20% to 0.63%, the graphene/epoxy nanocomposite has a dramatic transition from an insulator into a

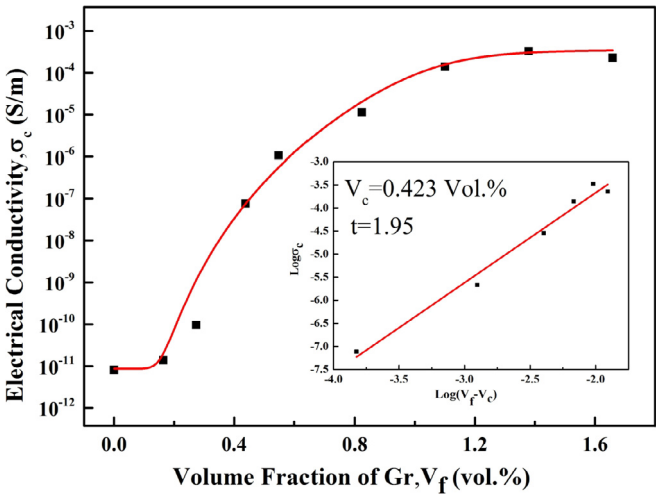

Fig. 9. The electrical conductivity versus conductive filler content for graphene/epoxy nanocomposites. The inset shows a double-logarithmic plot of electrical conductivity versus (V_f-V_c). Red lines correspond to the least square fitting of the experimental data.

semiconductor. Whereas the conductivity of the composite after adding graphene of 1.0 vol% or more reaches a high value in a level of 10^{-4} S/m. The electrical conductivity of the composites has clearly been increased by seven orders of magnitude, which is good enough for being used as an anti-static material or electromagnetic shielding material [41].

According to the percolation threshold theory [42], the conductivity of the polymer will be changed at a certain critical value as the content of the conductive filler is further increased. At this critical content, the conductive filler will form a conducting network inside the matrix to enhance the conductive properties of the composite. Although a lower amount of graphene (e.g., 0.3 wt%) dispersed in the matrix can effectively improve the mechanical properties of the composite [21], the graphene in the matrix at this low concentration cannot be effectively and uniformly connected in a large area, therefore, the conductivity values are not apparently improved.

The percolation threshold of graphene/epoxy composites can be estimated using the percolation theory based on the following equation [9,43,44]:

$$\sigma_c = \sigma_{gr}[\frac{(V_f - V_c)}{(1 - V_c)}] \qquad V_f > V_c \tag{6}$$

where V_f is the graphene's volume fraction and V_c is the percolation volume fraction, and σ_c and σ_{gr} are the conductivity values of the composite and the graphene, respectively. Moreover, t is the critical power law exponent. As is shown in the inset of Fig. 9, the best fitting of the experimental conductivity values to the log–log plots of the power laws gives the readings of $V_c = 0.423$ vol% and $t = 1.95$. These threshold values are much lower than those reported values for the graphene/epoxy composites [45].

When the content of graphene is increased above 2.0 wt%, the electrical conductivity of the composites has not been further increased. When the content of graphene is further increased up to 3.0 wt%, it even decreases slightly. From the cross-sectional TEM images of the composites (see Fig. 8(e)), when the content of graphene is 0.8 wt%, there are some agglomerates in the composite matrix. The agglomeration of graphene in the non-conductive epoxy resin matrix will not contribute much to the enhancement of conductivity. Therefore, the reason for the decrease in the conductivity of composites with a large graphene loading is mainly the agglomeration of graphene.

4. Conclusions

In this work, graphene/epoxy resin composites were prepared using *in-situ* polymerization with graphene as the filler and E-44 epoxy resin as the matrix. The following conclusions were obtained from this study:

(1) The hydroxyl groups on the surface of the graphene chemically reacts with the epoxy matrix and forms aliphatic ether, and there are covalent bonds formed between the graphene and the epoxy resin matrix. The interaction between the graphene and the matrix allows the graphene to be uniformly dispersed in the epoxy matrix.
(2) With the increase of graphene mass fraction, the mechanical properties of graphene/epoxy resin composites increase initially but then decrease. When the amount of graphene loading is 0.3 wt%, the composite material has the best mechanical properties. Compared with pure epoxy resin, its tensile strength, elastic modulus and elongation at break are increased by 46.8%, 47.3% and 24.0%, respectively. The improvement of the mechanical properties of composites is due to the dispersion strengthening and effective transfer of stress due to the graphene.
(3) The addition of graphene enhances the electrical conductivity of the composite. When the content of graphene is 1.38 vol%, the electrical conductivity of the composite is increased by seven orders of magnitude compared to the pure epoxy resin, reaching a maximum value of 3.28×10^{-4} S/m with a low percolation threshold of 0.47 vol%.

Acknowledgements

The authors would like to acknowledge the financial supports from Key Research and Development Projects of Shaanxi Province (No. 2017ZDXM-GY-050) and Electrical Materials and Infiltration Key Laboratory of Shaanxi Province Projects (No.17JS080), UK Engineering and Physical Sciences Research (EPSRC, EP/P018998), Newton Mobility Grant (IE161019) through Royal Society and the National Natural Science Foundation of China, and Royal academy of Engineering UK-Research Exchange with China and India. Scientific Research Program of Northwest Institute for Nonferrous Metal Research (K1652-1).

References

[1] D.A. Bolon, Epoxy chemistry for electrical insulation, IEEE Electr. Insul. Mag. 11 (4) (2002) 10–18.
[2] R.S. Bauer, Epoxy Resin Chemistry, American Chemical Society, 1979.
[3] Q. Li, Y. Guo, W. Li, S. Qiu, C. Zhu, X. Wei, et al., Ultrahigh thermal conductivity of assembled aligned multilayer graphene/epoxy composite, Chem. Mater. 26 (15) (2012) 4459–4465.
[4] M. Lei, B. Xu, Y. Pei, H. Lu, Y.Q. Fu, Micro-mechanics of nanostructured carbon/shape memory polymer hybrid thin film, Soft Matter 12 (1) (2016) 106–114.
[5] A.K. Geim, K.S. Novoselov, The rise of graphene, Nat. Mater. 6 (3) (2007) 183–191.
[6] J. Chen, C. Jang, S. Xiao, M. Ishigami, M. Fuhrer, Intrinsic and Extrinsic performance limits of graphene device on SiO_2, Nat. Nanotechnol. 3 (4) (2008) 206–209.
[7] J.C. Meyer, A.K. Geim, M.I. Katsnelson, K.S. Novoselov, T.J. Booth, S. Roth, The structure of suspended graphene sheets, Nature 446 (7131) (2007) 60–63.
[8] Y. Zhu, S. Murali, W. Cai, X. Li, J.W. Suk, J. Potts, et al., Graphene and graphene oxide: synthesis, properties, and applications, Adv. Mater. 22 (46) (2010) 3906–3924.
[9] D. Li, R.B. Kaner, Graphene-based materials, Science 320 (5880) (2008) 1170–1171.
[10] Y. Li, H. Zhang, H. Porwal, Z. Huang, E. Bilotti, T. Peijs, Mechanical, electrical and thermal properties of in-situ exfoliated graphene/epoxy nanocomposites, Compos. Pt. A-Appl. Sci. Manuf. 95 (2017) 229–236.
[11] Z. Liu, D. Shen, J. Yu, W. Dai, C. Li, S. Du, et al., Exceptionally high thermal and electrical conductivity of three dimensional graphene foam based polymer composites, RSC Adv. 6 (27) (2016) 22364–22369.
[12] H.J. Salavagione, G. Martínez, G. Ellis, Recent advances in the covalent modification of graphene with polymers, Macromol. Rapid Commun. 32 (22) (2011) 1771–1789.
[13] C. Chen, S. Qiu, M. Cui, S. Qin, G. Yan, H. Zhao, et al., Achieving high performance corrosion and wear resistant epoxy coatings via incorporation of noncovalent functionalized graphene, Carbon 114 (2017) 356–366.
[14] H. Yao, S.A. Hawkins, H.J. Sue, Preparation of epoxy nanocomposites containing well-dispersed graphene nanosheets, Compos. Sci. Technol. 146 (2017) 161–168.
[15] M.A. Milani, D. González, R. Quijada, N.R.S. Basso, M.L. Cerrada, D.S. Azambuja, et al., Polypropylene/graphene nanosheet nanocomposites by in situ, polymerization: synthesis, characterization and fundamental properties, Compos. Sci. Technol. 84 (2013) 1–7.
[16] M. Stürzel, F. Kempe, T. Yi, S. Mark, M. Enders, R. Mülhaupt, Novel graphene uhmwpe nanocomposites prepared by polymerization filling using single-site catalysts supported on functionalized graphene nanosheet dispersions, Macromolecules 45 (17) (2012) 6878–6887.
[17] J.R. Potts, H.L. Sun, T.M. Alam, J. An, M.D. Stoller, R.D. Piner, et al., Thermomechanical properties of chemically modified graphene/poly(methyl methacrylate) composites made by in situ polymerization, Carbon 49 (8) (2011) 2615–2623.
[18] D.X. Zhang, L.N. Huang, Polymer Matrix Composites Science and Engineering, Harbin Institute of Technology Press, Harbin, 2017, pp. 111–115 (in Chinese).
[19] J. Sarabadani, A. Naji, R. Asgari, R. Podgornik, Many-body effects in the van der waals-casimir interaction between graphene layers, Phys. Rev. B 84 (15) (2011) 3401–3408.
[20] L.L. Dong, W.G. Chen, N. Deng, C.H. Zheng, A novel fabrication of graphene by chemical reaction with a green reductant, Chem. Eng. J. 306 (2016) 754–762.
[21] D.G. Papageorgiou, I.A. Kinloch, R.J. Young, Mechanical properties of graphene and graphene-based nanocomposites, Prog. Mater. Sci. 90 (2017) 75–127.
[22] S. Guo, S. Dong, Graphene nanosheet: synthesis, molecular engineering, thin film, hybrids, and energy and analytical applications, Chem. Soc. Rev. 40 (5) (2011) 2644–2672.
[23] H. Kim, A.A. Abdala, C.W. Macosko, Graphene/polymer nanocomposites, Macromolecules 43 (16) (2010) 6515–6530.
[24] H. Kim, Y. Miura, C.W. Macosko, Graphene/polyurethane nanocomposites for improved gas barrier and electrical conductivity, Chem. Mater. 22 (11) (2010) 3441–3450.
[25] C.J. Shih, M.S. Strano, D. Blankschtein, Wetting translucency of graphene, Nat.

Mater. 12 (10) (2013) 866–869.
[26] R.S. Bauer, S. Ronald, Epoxy Resin Chemistry II, American Chemical Society, 1983.
[27] A.C. Ferrari, J.C. Meyer, V. Scardaci, C. Casiraghi, M. Lazzeri, F. Mauri, et al., Raman spectrum of graphene and graphene layers, Phys. Rev. Lett. 97 (18) (2006) 187401.
[28] L.L. Dong, W.G. Chen, N. Deng, J.L. Song, J.J. Wang, Investigation on arc erosion behaviors and mechanism of w70cu30 electrical contact materials adding graphene, J. Alloy. Comp. 696 (2016) 923–930.
[29] W.G. Chen, L.L. Dong, J.J. Wang, Y. Zuo, S.X. Ren, Y.Q. Fu, Synergistic enhancing effect for mechanical and electrical properties of tungsten copper composites using spark plasma infiltrating sintering of copper-coated graphene, Sci. Rep. 7 (1) (2017) 1–9.
[30] S. Stankovich, R.D. Piner, S.B.T. Nguyen, R.S. Ruoff, Synthesis and exfoliation of isocyanate-treated graphene oxide nanoplatelets, Carbon 44 (15) (2006) 3342–3347.
[31] S. Park, K.S. Lee, G. Bozoklu, W. Cai, S.T. Nguyen, R.S. Ruoff, Graphene oxide papers modified by divalent ions-enhancing mechanical properties via chemical cross-linking, ACS Nano 2 (3) (2008) 572–578.
[32] S. Park, D.A. Dikin, S.B.T. Nguyen, R.S. Ruoff, Graphene oxide sheets chemically cross-linked by polyallylamine, J. Phys. Chem. C 113 (36) (2009) 15801–15804.
[33] Q.Y. Xing, W.W. Pei, R.Q. Xu, J. Pei, Basic Organic Chemistry, Higher Education Press, Beijing, 2005, p. 180 (in Chinese).
[34] M.B. Smith, J. March, March's Advanced Organic Chemistry: Reactions, Mechanisms, and Structure, fifth ed., John Wiely & Sons, Hoboken, 2007, p. 236.
[35] Y. Zhang, Y. Wang, J. Yu, L. Chen, J. Zhu, Z. Hu, Tuning the interface of graphene platelets/epoxy composites by the covalent grafting of polybenzimidazole, Polymer 55 (19) (2014) 4990–5000.
[36] Y. Ni, L. Chen, K. Teng, J. Shi, X. Qian, Z. Xu, et al., Superior mechanical properties of epoxy composites reinforced by 3D interconnected graphene skeleton, ACS Appl. Mater. Interfaces 7 (21) (2015) 11583–11591.
[37] J.C. Halpin, Effect of Environmental Factors on Composite Materials, DTIC document, 1969.
[38] J.A. King, D.R. Klimek, I. Miskioglu, G.M. Odegard, Mechanical properties of graphene nanoplatelet/epoxy composites, J. Appl. Polym. Sci. 128 (6) (2013) 4217–4223.
[39] M.A. Rafiee, RafieeJ, Z. Wang, H. Song, Z.Z. Yu, N. Koratkar, Enhanced mechanical properties of nanocomposites at low graphene content, ACS Nano 3 (12) (2009) 3884–3890.
[40] H.B. Zhang, W.G. Zheng, Q. Yan, Y. Yang, J.W. Wang, Z.H. Lu, et al., Electrically conductive polyethylene terephthalate/graphene nanocomposites prepared by melt compounding, Polymer 51 (2010) 1191–1196.
[41] J. Liang, Y. Wang, Y. Huang, Y. Ma, Z. Liu, J. Cai, et al., Electromagnetic interference shielding of graphene/epoxy composites, Carbon 47 (3) (2009) 922–925.
[42] I.A. Tchmutin, A.T. Ponomarenko, V.G. Shevchenko, N.G. Ryvkina, C. Klason, D.H. Mcqueen, Electrical transport in 0-3 epoxy resin-barium titanate-carbon black polymer composites, J. Polym. Sci. B Polym. Phys. 36 (11) (2015) 1847–1856.
[43] F. He, S. Lau, H.L. Chan, J.T. Fan, High dielectric permittivity and low percolation threshold in nanocomposites based on poly(vinylidene fluoride) and exfoliated graphite nanoplates, Adv. Mater. 21 (2009) 710–715.
[44] L. Bai, S.Y. He, J.W. Fruewirth, A. Stein, C.W. Macosko, X. Chen, Localizing graphene at the interface of cocontinuous polymer blends: morphology,rheology, and conductivity of cocontinuous conductive polymer composites, J. Rheol. 61 (2017) 575–587.
[45] A.J. Marsden, D.G. Papageorigiou, C. Valles, A. Liscio, V. Palermo, M.A. Bissett, et al., Electrical percolation in graphene–polymer composites, 2D Mater. 5 (2018) 1–19.